A unified molecular picture of the surfaces of aqueous acid, base, and salt solutions

Martin Mucha,[1] Tomaso Frigato,[1,2] Lori Levering,[3] Heather C. Allen,[3] Douglas J. Tobias,[4] Liem X. Dang,[5] and Pavel Jungwirth[1*]

(1) Institute of Organic Chemistry and Biochemistry, Academy of Sciences of the Czech Republic, and Center for Complex Molecular Systems and Biomolecules, Flemingovo nám. 2, 16610 Prague 6, Czech Republic,

(2) Max Planck Institute for Biophysics, Marie Curie Str. 15, D-60439, Frankfurt am Main, Germany,

(3) Department of Chemistry, The Ohio State University, 100 W. 18th Ave., Columbus, Ohio 43210, USA,

(4) Department of Chemistry and Institute for Surface and Interface Science, University of California, Irvine, CA 92697-2025, USA,

(5) Chemical Sciences Division, Pacific Northwest National Laboratory, Richland, WA 99352, USA

[*]Corresponding author (e-mail: pavel.jungwirth@uochb.cas.cz).

Abstract

The molecular structure of the interfacial regions of aqueous electrolytes is poorly understood, despite its crucial importance in many biological, technological, and atmospheric processes. A long-term controversy pertains between the standard picture of an ion-free surface layer and the strongly ion specific behavior indicating in many cases significant propensities of simple inorganic ions for the interface. Here, we present a unified and consistent view of the structure of the air/solution interface of aqueous electrolytes containing monovalent inorganic ions. Molecular dynamics calculations show that in salt solutions and bases the positively charged ions, such as alkali cations, are repelled from the interface, while the anions, such as halides or hydroxide, exhibit a varying surface propensity, correlated primarily with the ion polarizability and size. The behavior of acids is different due to a significant propensity of hydronium cations for the air/solution interface. Therefore, both cations and anions exhibit enhanced concentrations at the surface and, consequently, these acids (unlike bases and salts) reduce the surface tension of water. The results of the simulations are supported by surface selective non-linear vibrational spectroscopy, which reveals among other things that the hydronium cations are present at the air/solution interface. The ion specific propensities for the air/solution interface have important implications for a whole range of heterogeneous physical and chemical processes, including atmospheric chemistry of aerosols, corrosion processes, and bubble coalescence.

1. Introduction

The traditional view of inorganic aqueous salt solution surfaces being devoid of ions[1-3] is yielding gradually to a more complex picture, where ion specificity plays a crucial role[4]. Small, non-polarizable (hard) ions (e.g., alkali cations and fluoride anions) are repelled from the air/solution interface by the electrostatic image forces, as described already by Onsager and Samaras in the 1930s[1]. However, polarizable (soft) ions, such as the heavier halides, nitrate, or azide, exhibit a propensity for the air/solution interface. This surprising fact, predicted by molecular dynamics simulations[5-8] and supported by various surface sensitive spectroscopic and electron microscopy measurements[9-13] is not in contradiction with basic thermodynamic arguments based on the Gibbs adsorption equation[2]. Simple inorganic salts raise the surface tension of water, from which an integral net depletion of ions from the interfacial region (i.e., negative surface excess) is inferred[3]. This, however, does not exclude a non-monotonous ion concentration profile with surface enhancement and sub-surface depletion, as observed qualitatively in the simulations, e.g., for bromide and iodide salt solutions[5,14]. It has been shown that such surface ion enhancement can have important atmospheric consequences, for example for the heterogeneous chemistry of seawater aerosols or for tropospheric ozone destruction in the Arctic and Antarctic at polar sunrise due to reactions involving sea spray covered ice pack[4,15].

Aqueous salt solutions are, however, only one third of the story concerning the surfaces of electrolytes. It has been known for a long time that salts and bases increase surface tension of water, while adding appreciable amounts of monovalent inorganic acids decrease it [3,16]. However, few experiments have been devoted to the molecular structure of the surfaces of concentrated aqueous acids and bases[17-20]. The

corresponding molecular simulations are lacking almost completely, with the notable exception of a recent pioneering study of a single proton and chloride at the extended air/water interface.[21] The present paper aims to close this gap by reporting detailed molecular dynamics (MD) simulations in slab geometries complemented by surface selective vibrational sum frequency generation (VSFG) spectroscopy of generic concentrated acid, base, and salt solutions. A unified picture with molecular resolution of the air/solution interface of simple aqueous inorganic electrolytes is emerging. Within this picture, hydronium cations and large polarizable anions exhibit a propensity for the interface, in contrast with the traditional view of an ion-free surface layer. This new view not only allows us to rationalize seemingly contradictory macroscopic surface measurements, but also has important implications for a variety of heterogeneous chemical processes, e.g., in the atmosphere.[15,22]

2. Computational method

The air/solution interface was modelled via 1 ns molecular dynamics simulations (after 500 ps of equilibration) at 300 K of water slabs containing HCl, HBr, NaOH, or NaCl at 1.2 M, and HI or NaI at 1.0 M concentration. Simulations in slab geometry were performed using the AMBER (versions 6 and 7) program package[23] with polarizable potentials both for water (POL3[24] and, in the cases of aqueous HI and NaI, DC97[25]) and the alkali, halide, hydronium, and hydroxide ions[5,6,26-28]. The induced electric field was converged in each step using a self-consistent procedure (the convergence was tighter than in our older simulations, which is the main reason for slightly different results for NaCl compared to those obtained previously[4,5]). For aqueous OH^-, where charge transfer effects can be

important and, consequently, a classical force field should be employed carefully, we tested a whole range of potential parameters with van der Waals radii of oxygen ranging from 1.8 to 2.1 A and polarizabilities between 1.8 and 3 A^3. Although the quantitative details of the results depended on the particular parameterization, the weak repulsion of hydronium anions from the interface was robustly reproduced in all cases. In addition to the classical force field model of H_3O^+ (which should also be used with care since it, e.g., does not allow for proton hopping and for the appearance of the Zundel form) we also employed a quantum hopping model of the hydrated proton[29]. The latter model, which accounts for proton hops between water molecules in a stochastic way, resulted in almost the same surface propensity of hydronium as for the non-polarizable version of the classical potential[28].

A slab of 864 (1000 in the cases of aqueous HI and NaI) water molecules was used to construct each system by adding 18 cations and 18 anions. Each slab was placed into a 30 x 30 x 100 A^3 (32 x 32 x 135 A^3 in the cases of aqueous HI and NaI) rectangular box, and periodic boundary conditions were applied in three dimensions. For this size of a simulation box we can interchangeably talk about air/solution and vacuum/solution interface, since at atmospheric pressure the number of nitrogen or oxygen molecules in the unit box is negligible[4]. Note that at these salt concentrations there is only a very small tendency of forming contact ion pairs, both in the bulk and at the interface[30]. The simulations were run at a constant temperature of 300 K. The smooth particle mesh Ewald method[31] was used to calculate the long range electrostatic energies and forces, and the van der Waals interactions and the real space part of the Ewald sum were truncated at 12 A. A time step of 1 fs was used in the integration of the equations of motion, and the OH bond vibrations were frozen using the SHAKE algorithm[32].

3. Experimental method

The experimental setup of the vibrational SFG scanning system has been described previously[10]. The SFG experiments were carried out using a visible beam at 532 nm and an infrared beam currently tunable from 2500 to 4000 cm^{-1} with a bandwidth of ~8 cm^{-1} generated from a KTP-KTA based optical parametric generator/amplifier (OPG/OPA) system (LaserVision). The 532 nm beam is generated by doubling the frequency (second harmonic) of the 1064 nm pump source from an EKSPLA PL 2143 A/SS Nd:YAG laser (29 ps pulse duration and 10 Hz repetition rate). The energies of the 532 nm and the infrared beams at the sample are ~1.1 mJ and ~350 μJ, respectively. The SFG signal is filtered from the reflected 532 nm light and detected with a charge-coupled device (CCD) (Andor Technology, DV412). The input angles are ~45^{o} and ~53^{o} for the 532 nm and IR beams respectively from the surface normal; the detection angle was set to ~ 46^{o} from the surface normal for sum frequency. The CCD temperature was set at -42 °C during the experiments and was cooled thermoelectrically.

All of the spectra presented in this paper were acquired in ~60 min using a 20 s exposure time for each data point (from 2800 to 3950 cm^{-1}). VSFG spectra were reproduced several times over the period of several months. Each free OH spectrum (Fig. 4 inset) is an average of three spectra and error bars are one standard deviation. At least one air-neat water spectrum was acquired at the beginning and the end of the experiment to ensure the stability of the SFG system and to confirm reproducibility.

The SFG signal is optimized spatially and temporally at 3300 cm^{-1}. The VSFG spectra are normalized by the IR profile since the IR is detected in real time with the SFG intensity. (The SFG spectrum was also obtained from the surface of a GaAs crystal, and was comparable to the IR spectrum.) The polarization combination used for the SFG experiments presented here are s, s, and p for the SFG, 532 nm, and infrared beams, respectively. However, additional polarization spectra were obtained and confirmed lack of orientation changes. All VSFG spectra were acquired at ~23 °C.

Water was obtained from a Millipore Nanopure system (18.3 MΩ·cm). Acid solutions were made volumetrically from concentrated HCl (Fisher Scientific, 36.5 wt. %,), HBr (Fisher Scientific, 48 wt. %) and HI (Alfa Aesar, 47 wt. %). All of the acid solutions were checked for organic contamination by obtaining the SFG spectra of the solution surfaces in the region between 2800 and 3000 cm^{-1}. To prevent the HI solutions from reaction with light, solutions were stored in a dark cabinet and the flasks were covered with aluminium foil.

4. Computational results

The structure of air/solution interfaces of solutions of generic inorganic salts (sodium chloride and iodide), base (sodium hydroxide), and acids (hydrochloric, hydrobromic, and hydroiodic acid) was investigated by means of MD simulations. The details concerning the calculations are provided in the Methods section. Briefly, extended slabs of concentrated aqueous solutions of HCl, HBr, NaOH, NaCl, NaI, or HI containing a bulk region between two air/solution interfaces were modelled using

periodic boundary conditions with a prismatic unit cell[4,33]. A polarizable force field was employed both for water and for the $H3O^+$, Na^+, Cl^-, Br^-, I^- and OH^- ions. Nanosecond-length simulations at ambient conditions of well equilibrated systems ensured adequate sampling of structural properties.

The principal results of the MD simulations of aqueous 1.2 M solutions of HCl, HBr, NaOH, and NaCl are summarized in Fig. 1. For each of the four solutions we show the density profiles (i.e., averaged distributions of electrolyte ions and water molecules from the bulk region of the slab to the interface) together with typical snapshots from the simulations, depicting top and side views of the systems. Note that in our concentrated systems monitoring the distributions of ions of each type in the slab provides much better statistics than one would get from a potential of mean force of a single ion.

In the case of hydrochloric acid both hydronium cations and chloride anions penetrate into the air/solution interface, and there is actually a slight surface ion enhancement of both ions. For hydrobromic acid the situation is similar, except that bromide is more surface enhanced than chloride or hydronium. Note that the hydronium cations are preferentially oriented at the surface, with hydrogens pointing towards the aqueous phase and oxygen towards the air.

The surface behavior of ions is very different in sodium hydroxide and sodium chloride solutions. On one hand, in aqueous NaOH and NaCl sodium cations are repelled from the surface and never penetrate its topmost layer. On the other hand, hydroxide anions are weakly repelled from and chloride anions weakly attracted to the surface, and both can be found at the surface. We mention in passing that the

orientation of OH^- at the surface, with hydrogen pointing into the gas phase (as in the snapshot shown in Fig. 1) nicely matches that observed in water clusters[34].

The effect of added electrolyte on the surface tension of aqueous solutions has been intensely studied for almost a century[35]. Although surface tension measurements do not give direct information about the molecular structure of the surface, they yield, via the Gibbs adsorption equation, information about the net excess of ions in the whole interfacial layer[2]. If surface tension increases compared to neat water, this excess is negative (indicating a net depletion of ions from the interface), while a decrease in surface tension is related to a positive surface excess (i.e., a net enrichment of ions in the interfacial layer). It has been known for decades that salts such as alkali halides and bases such as alkali hydroxides increase the surface tension of water, while acids such as HCl, HBr, or HI slightly decrease it[3].

Surface tension can be extracted from MD simulations, albeit with a sizable statistical error due to large pressure fluctuations, from the asymmetry of the pressure tensor[36]. Despite the fact that the calculated numbers are subject to statistical errors of at least 1 mN/m, the experimental trend[3] is reproduced by the present simulations. Namely, on one hand the calculated surface tension of 1.2 M HCl is within the statistical error equal to that of neat water, while that of 1.2 M HBr is smaller by about 1 mN/m. Note, that no ion association into a molecular acid is invoked in the simulation to account for the decrease of surface tension, in agreement with the anticipated complete dissociation of these strong acids at molar concentrations, confirmed by earlier VSFG measurements[17]. On the other hand, both 1.2 M NaOH and 1.2 M NaCl increase the surface tension, the calculated numbers being ~4 mN/m in the former case and ~3 mN/m in the latter case. Interestingly, all the investigated

systems exhibit the same polarity of the surface potential (negative towards the air)[3]. While for NaCl and NaOH this is primarily due to the fact that anions reside closer to the interface than cations, for HCl and HBr there is also a contribution from the hydronium ions which have the electronegative oxygen atom oriented toward the gas phase.

We carried out additional simulations to compare the solvation properties of 1 M HI or NaI at the air/solution interface. In the case of aqueous HI, hydronium is present both in the bulk and at the interface (with appreciable surface enhancement) and iodide exhibits a surface concentration peak, which is larger than that for the lighter halides. In aqueous NaI sodium is repelled from the top surface layer, albeit less than in the case of NaCl, which is due to attractive cation-anion interactions and the stronger surface propensity of iodide compared to chloride. The iodide density profiles for aqueous HI and NaI are plotted in Fig. 2. It can be seen from this figure that for HI the interfacial peak of iodide is about 10 % larger and shifted by more than 1 A toward the gas phase, compared to that in the NaI solution. This is in perfect agreement with most recent Second Harmonic Generation spectroscopic measurements[20], showing an enhanced interfacial iodide signal upon moving from aqueous NaI to HI.

The picture emerging from the simulations is that monovalent inorganic acids have different surface behavior from the corresponding salts and bases in aqueous solutions. In acids both the hydronium cations and the anions exhibit a propensity for the air/solution interface. While the affinity of H_3O^+ for the surface is relatively weak, anions exhibit specificity that correlates with the ion polarizability and size. Br^- and I^- (as well as, e.g., N_3^- or NO_3^-)[7-8,11] show a stronger surface enhancement, while the

surface propensity of Cl^- is comparable to that of H_3O^+. As a result of the surface propensity of both cations and anions in aqueous HCl, HBr, or HI, there is a net positive surface excess of ions. In bases and salt solutions, the cations, which are small and non-polarizable spherical ions, are repelled from the surface. OH^- penetrates closer to the surface than alkali cations and can be occasionally found in the topmost layer but it does not exhibit any appreciable enhancement at the air/solution interface. The salt anions exhibit ion specific degrees of surface enhancement, similarly as in the case of the corresponding acids. The result of strong cationic repulsion and varying anionic surface propensity is a net depletion of ions from the interfacial layer of aqueous salt solutions and bases.

To connect the simulations to the spectroscopic experiments, we have computed the surface density (number per unit area) of free OH bonds, , i.e. OH bonds not serving as hydrogen bond donors, where water-water and water-ion hydrogen bonds have been defined using a geometric criterion[5]. The results for neat water, 1.2 M HCl, HBr, NaOH, and NaCl are shown in Fig. 3. In all systems the density of free OH bonds is higher in the interfacial region than in the bulk. While the density of free OH bonds in the interfacial region is about the same for neat water, NaOH, and NaCl, it is significantly reduced for the two acids, in accord with the spectroscopic data presented next.

5. Experimental results

Vibrational sum frequency generation spectroscopy (VSFG) is a second-order vibrational spectroscopic technique that is selective to environments lacking inversion

symmetry such as interfaces and is used here to directly probe the air/solution interface.[10,17-19,37] The VSFG surface spectra for 1.2 M HCl, HBr, HI, NaOH, and NaCl are shown in Fig. 4 under ssp polarization conditions (s and p are perpendicular and parallel to the plane of incidence, respectively), which provide information on molecular orientations[38], when quantitatively compared to sps VSFG spectra which showed no signal beyond the noise.

The spectra in Fig. 4 reveal very different interfacial behavior for the acids versus sodium hydroxide and sodium halide solutions. The VSFG spectrum of neat water is also shown for comparison. Based on the IR and Raman spectra of aqueous acid solutions, the additional VSFG intensity below 3200 cm^{-1} for the HCl, HBr, and HI solutions as compared to the neat water surface spectrum is attributed to VSFG response from hydronium (Eigen) and Zundel cations[39]. The intensity of the 3400 cm^{-1} band, which is assigned to oscillating dipoles about the tetra-coordinated interfacial water molecules in these acid solutions, increases relative to neat water, with $I^- \sim Br^- > Cl^-$. In the 3700 cm^{-1} region, the sharp peak assigned to the dangling OH of water molecules that straddle the air/solution interface decreases for the acids (Fig. 4 inset) relative to neat water, although there is a small increase on the higher energy side next to this peak. The 3400 cm^{-1} band increase is consistent with our previous results on sodium halide air/solution interfaces, which indicated that the halides play a dominant role in influencing the 3400 cm^{-1} band similar to observations from Raman spectroscopy of the bulk salt solutions[10]. However, the 3100 cm^{-1} band increases and the 3700 cm^{-1} peak decreases are unique to the acids, and are not observed for the base (sodium hydroxide) and the sodium salt air/solution interfaces.

Consistent with the MD simulations, the VSFG data reveal that protonated water exists in the interfacial region. The observed decrease in the dangling OH intensity for HCl and HBr as shown in the inset of Fig. 4 is also consistent with the decrease in free OH number densities derived from the MD simulates as stated above (see Fig. 3). Changes in the orientation distribution have been ruled out from VSFG polarization data; this is consistent with water dipole orientational distributions calculated from the simulations, which are essentially the same in all the systems considered. The absence of VSFG intensity increases from the aqueous sodium hydroxide surface is consistent with the MD simulations showing a net depletion of OH^- at the surface (see Fig. 1). Evidently, spectroscopic experiments and molecular simulations are converging to a unified picture of the interfacial structure of simple electrolyte solutions.

6. Discussion and broader implications

The bottom line of the present study is that on one side there are monovalent inorganic acids, where both cations and anions exhibit a propensity for the air/solution interface, while on the other side in bases and salt solutions cations are repelled from the interface and anions show a varying surface affinity. Thus, the distinguishing feature is the different surface behavior of hydronium compared to that of other cations. Atomic cations such as alkali ions practically do not penetrate the topmost layer of aqueous solutions. Hydronium cation behaves differently, primarily due to the "hydrophobic" character of its oxygen.[21] While the three hydrogens of H_3O^+ are good hydrogen bond donors, the oxygen is, due to a significantly reduced negative charge (-0.4 e compared to a charge of -0.8 e of water oxygen), a relatively poor

hydrogen bond acceptor. As a result of its amphiphilic character (a term coined in Ref. 21), hydronium can be stabilized at the air/solution interface with its H atoms hydrogen bonded to surrounding water molecules, while its oxygen atom remains unbound and pointing into the gas phase. This preferential orientation of H_3O^+ at the air/solution interface of aqueous HCl and HBr, as extracted from our simulations, is plotted in Fig. 5.

We have verified the above predictions of classical molecular dynamics by a non-polarizable quantum hopping molecular dynamics (Q-HOP MD) simulation[29] for a single proton in an aqueous slab. Fig. 6a) shows a comparison between density profiles of a single proton and single sodium cation in aqueous slabs (the inferior statistics in Fig. 6 compared to Fig. 1 is due to sampling over a single ion only). These non-polarizable calculations confirm that the proton (unlike the sodium cation) penetrates into the interfacial layer, and its density profile across the slab almost coincides with that of a single hydronium in a water slab, described by a classical non-polarizable force field (see Fig. 6b). The addition of polarizability of hydronium and water leads to a further increase of the surface propensity of H_3O^+, as shown in Fig. 6b. These results are in perfect agreement with the most recent quantum calculations, which show the surface propensity of a single proton in aqueous clusters and slabs[21,40-41].

Recently, the surface of ice doped with NaCl or HCl has been investigated in detail by means of cesium ion sputtering[42-43]. Upon heating the ice the two systems behave very differently from each other. While in the case of NaCl doped ice heating results in the disappearance of sodium cations (but not chloride anions) from the surface[43], in the case of HCl doped ice the elevation of temperature leads to a cationic

(i.e., hydronium) and anionic surface enrichment[42]. Despite the fact that these experiments concern ice surfaces, the vastly different behavior of salt vs. acid doped systems is indicative also for air/solution interfaces.

The results of the present calculations may shed some light on a long standing problem of the effect of electrolyte on bubble coalescence[44-46]. While simple inorganic salts tend to inhibit bubble coalescence (which is one of the reasons why foam is formed when waves break in the ocean but not in fresh water lakes) the corresponding acids have no effect[44-45]. It is conceivable that the inhibition of bubble coalescence is related to Coulomb repulsion between interfaces due to separation of cations and anions at the air/solution interface of salts, such as alkali chlorides, bromides, iodides, or nitrates. Due to the surface propensity of hydronium, strong charge separation is not observed at the interfaces of aqueous HCl, HBr, HI, or HNO_3.

Inorganic electrolytes containing multivalent ions are beyond the scope of the present study, but they nevertheless deserve a brief remark. It has been shown both in experiments and calculations, that multiply charged inorganic ions are always very strongly repelled from the air/solution interface due to very strong ion-water electrostatic interactions, even when the ion is very polarizable (such as sulfate)[47-48]. Taking as an example sulfuric acid, it has been known for a long time that H_2SO_4 increases surface tension at low concentrations, but decreases it at high concentrations[16]. This non-monotonous behavior of surface tension and, consequently, of the surface excess can be rationalized within the picture emerging from the present study. Namely, at low concentrations, H_2SO_4 is predominantly dissociated to hydronium and SO_4^{2-} ions. In this situation the weak attraction of hydronium to the surface cannot compete with the strong repulsion of sulfate dianion

from the air/solution interface. This results in a net negative surface ion excess (i.e., net depletion of ions from the interface) and, consequently, a surface tension increase. At higher concentrations, H_2SO_4 is no longer fully dissociated and HSO_4^- is becoming the predominant anion. Being a soft monovalent anion, bisulfate is not strongly repelled from the air/solution interface[14]. This allows for a build up of a positive net surface ion excess (i.e., net enrichment of ions in the interfacial layer) resulting in a surface tension decrease. Moreover, H_2SO_4, which is a weaker acid than HCl, HBr, or HI can presumably also appear at higher concentrations at the surface in a molecular form, and this could further contribute to the lowering of surface tension.

7. Summary

A new picture of the air/solution interface of simple inorganic electrolytes emerges from the present molecular dynamics calculations and VSFG spectroscopic experiments. In contradiction with the traditional view, ions can play an active role at the interface and strong ionic specificity in surface propensity is the key to understanding macroscopic properties at the molecular level. In particular, the opposite sign of the change in surface tension upon adding bases (e.g., alkali hydroxides) and salts (such as alkali halides) on one side, and the corresponding acids on the other side can be related to the much stronger propensity of hydronium for the air/solution interface, compared to alkali cations. While the present large scale molecular simulations necessarily employ a relatively simple polarizable classical force field (which can only approximately describe water molecules, salt ions and, in particular, hydroxide and hydronium) the results are robust and compare well with

more accurate calculations on benchmark systems, as well as with most of the surface selective experiments.

The present results not only suggest a conceptual change in the perception of the surfaces of electrolytes, which are still mostly described within the continuum dielectric models[49-52], but also have important practical implications for interfacial physical processes (such as bubble coalescence) and heterogeneous chemistry, e.g., in the atmosphere. For salts, this has already been recognized in studies of the chemistry of aqueous sea-salt aerosols[15,53-54], while for acids there is a plethora of hitherto unexplored effects, for example within the realm of the chemistry (e.g., corrosion processes) in the marine boundary layer or droplet and ice nucleation and cloud formation[55].

Acknowledgment

We thank B. J. Finlayson-Pitts and E. C. Brown for valuable comments. Support via the NSF-funded Environmental Molecular Science Institute (grant CHE 0431512) and from the Czech Ministry of Education (grant ME644) is gratefully acknowledged. Part of the work in Prague was supported via the Research Project Z40550506. The work at PNNL was performed under the auspices of the Division of Chemical Sciences, Office of Basic Energy Sciences, U. S. Department of Energy. Support of the experimental work at Ohio State by NSF (grant ATM-0413893) and Research Corporation (Research Innovation Award) is also gratefully acknowledged.

References

1. Onsager, L.; Samaras, N. N. T. *J. Chem. Phys.* **1934**, *2*, 528.

2. Adam, N. K. *The Physics and Chemistry of Surfaces*; Oxford University Press, London, 1941.

3. Randles, J. E. B. *Phys. Chem. Liq.* **1977**, *7*, 107.

4. Jungwirth, P.; Tobias, D. J. *J. Phys. Chem. B* **2002**, *106*, 6361.

5. Jungwirth, P.; Tobias, D. J. *J. Phys. Chem. B* **2001**, *105*, 10468.

6. Dang, L. X.; Chang, T.-M. *J. Phys. Chem. B* **2002**, *106*, 235.

7. Salvador, P.; Curtis, J. E.; Tobias, D. J.; Jungwirth, P. *Phys. Chem. Chem. Phys.* **2003**, *5*, 3752.

8. Yang, X.; Kiran, B.; Wang, X.-B.; Wang, L.-S.; Mucha, M.; Jungwirth, P. *J. Phys. Chem. A* **2004**, *108*, 7820.

9. Ghosal, S.; Shbeeb, A.; Hemminger, J.C. *Geophys. Res. Lett.* **2000**, *27*, 1879.

10. Liu, D.; Ma, G.; Levering, L. M.; Allen, H. C. *J. Phys. Chem. B* **2004**, *108*, 2252.

11. Petersen, P. B.; Saykally, R. J. *Chem. Phys. Lett.* **2004**, *397*, 51.

12. Petersen, P. B.; Johnson, J. C.; Knutsen, K. P.; Saykally, R. J. *Chem. Phys. Lett.* **2004**, *397*, 46.

13. Ghosal, S.; Requero, F.; Mun, B. S.; Ogletree, F.; Salmeron, M.; Hemminger, J. C., *submitted*.

14. Vrbka, L.; Mucha, M.; Minofar, B.; Jungwirth, P.; Brown, E. C.; Tobias, D. J. *Curr. Opp. Colloid Interface Sci.* **2004**, *9*, 67.

15. Knipping, E. M.; Lakin, M. J.; Foster, K. L.; Jungwirth, P.; Tobias, D. J.; Gerber, R. B.; Dabdub, D.; Finlayson-Pitts, B.-J. *Science* **2000**, *288*, 301.

16. Washburn, E. W. ed. *International Critical Tables, Vol. IV*, McGraw-Hill, New York, 1928.

17. Baldelli, S.; Schnitzer, C.; Shultz, M. J. *Chem. Phys. Lett.* **1999**, *302*, 157.

18. Baldelli, S.; Schnitzer, C.; Campbell, D. J.; Shultz, M. J. *J. Phys. Chem. B* **1999**, *103*, 2789.

19. Schnitzer, C.; Baldelli, S.; Campbell, D. J.; Shultz, M. J. *J. Phys. Chem. A* **1999**, *103*, 6383.

20. Petersen, P. B.; Saykally, R. J., *submitted*.

21. Petersen, M. K.; Iyengar, S. S.; Day, T. J. F.; Voth, G. A. *J. Phys. Chem. B* **2004**, *108*, 14804.

22. Foster, K. L.; Plastridge, R. A.; Bottenheim, J. W.; Shepson, J. B.; Finlayson-Pitts, B. J.; Spicer, C. W. *Science* **2001**, *291*, 471.

23. Case, D. A.; Pearlman, D. A.; Caldwell, J. W.; Cheatham III, T. E.; Ross, W. S.; Simmerling, C. L.; Darden, T. A.; Merz, K. M.; Stanton, R. V.; Cheng, A. L.; Vincent, J. J.; Crowley, M.; Tsui, M.; Radmer, R. J.; Duan, R. Y.; Pitera, J.; Massova, I.; Seibel, G. L.; Singh, U. C. *AMBER6*, University of California, San Francisco, 1999.

24. Caldwell, J.; Kollman, P. A. *J. Phys. Chem.* **1995**, *99*, 6208.

25. Dang, L. X.; Chang, T.-M. *J. Chem. Phys.* **1997**,*106*, 8149.

26. Dang, L. X.; *J. Phys. Chem. B* **2002**, *106*, 10398.

27. Brodskaya, E.; Lyubartsev, A. P.; Laaksonen, A. *J. Phys. Chem. B* **2002**, *106*, 6479.

28. Dang, L. X.; *J. Chem. Phys.* **2003**,*119*, 6351.

29. Liil, M. A.; Helms, V. *J. Chem. Phys.* **2001**,*115*, 7993.

30. Jungwirth, P.; Tobias, D. J. *J. Phys. Chem. B* **2000**,*104*, 7702.

31. Essmann, U.; Perera, L.; Berkowitz, M. L.; Darden, T. A.; Pedersen, L. G. *J. Chem. Phys.* **1995**, *103*, 8577.

32. Ryckaert, J.-P.; Ciccotti, G.; Berendsen, H. J. C. *J. Comp. Phys.* **1977**, *23*, 327.

33. Wilson, M. A.; Pohorille, A. *J. Chem. Phys.* **1991**, *95*, 6005.

34. Robertson, W. H.; Diken, E. G.; Price, E. A.; Shin, J.-W.; Johnson, M. A. *Science* **2003**, *299*, 1367.

35. Heydweiler, A. Ann. Phys. **1910**, *33*, 145.

36. Zhang, Y.; Feller, S. E.; Brooks, B. R.; Pastor, R. W. *J. Chem. Phys.* **1995**, *103*, 10252.

37. Raymond, E. A.; Richmond, G. L. *J. Phys. Chem. B* **2004**, *108*, 5051.

38. Moad, A. J.; Simpson, G. J. *J. Phys. Chem. B* **2004**, *108*, 3548.

39. Buch, V.; Sadlej, J.; Aytemiz-Uras, N.; Devlin, J. P. *J. Phys. Chem. A* **2002**, *106*, 9374.

40. Iyengar, S. S.; Day, T. J. F.; Voth, G. A. *Int. J. Mass Spectrometry, in press.*

41. Shin, J. W.; Hammer, N. I.; Diken, E. G.; Johnson, M. A.; Walters, R. S.; Jaeger, T. D.; Duncan, M. A.; Christie, R. A.; Jordan, K. D. *Science* **2004**, *304*, 1137.

42. Kang, H.; Shin, T.-H.; Park, S.-C.; Kim, I. K.; Han, S.-J. *J. Am. Chem. Soc.* **2000**, *122*, 9842.

43. Kim, J.-H.; Shin, T.; Jung, K. H.; Kang, H. *J. Chem. Phys.*, in press.

44. Craig, V. S. J.; Ninham, B. W.; Pashley, R. M. *Nature* **1993**, *364*, 317.

45. Craig, V. S. J. *Curr. Opp. Colloid Interface Sci.* **2004**, *9*, 178.

46. Marcelja, S. *Curr. Opp. Colloid Interface Sci.* **2004**, *9*, 165.

47. Wang, X.-B.; Yang, X.; Nicholas, J. B.; Wang, L.-S. *Science* **2001**, *294*, 1322.

48. Jungwirth, P.; Curtis, J. E.; Tobias, D. J. *Chem. Phys. Lett.* **2003**, *367*, 704.

49. Manciu, M.; Ruckenstein, E. *Adv. Colloid Interface Sci.* **2003**, *105*, 63.

50. Markin, V. S.; Volkov, A. G. *J. Phys. Chem. B* **2002**, *106*, 11810.

51. Karraker, K. A.; Radke, C. J. *Adv. Colloid Interface Sci.* **2002**, *96*, 231.

52. Bostrom, M.; Williams, D. R. M.; Ninham, B. W. *Langmuir* **2001**, *17*, 4475.

53. Finlayson-Pitts, B. J.; Hemminger, J. C. *J. Phys. Chem. A* **2000**, *104*, 11463.

54. Hu, J. H.; Shi, Q.; Davidovits, P.;Worsnop, D. R.; Zahniser, M. S.; Kolb, C. E. *J. Phys. Chem.* **1995**, *99*, 8768.

55. Gao, R. S.; Popp, P. J.; Fahey, D. W.; Marcy, T. P.; Herman, R. L.; Weinstock, E. M.; Baumgardner, D. G.; Garrett, T. J.; Rosenlof, K. H.; Thompson, T. L.; Bui, P. T.; Ridley, B. A.; Wofsy, S. C.; Toon, O. B.; Tolbert, M. A.; Kärcher, B.; Peter, T.; Hudson, P. K.; Weinheimer, A. J.; Heymsfield, A. J. *Science* **2004**, *303*, 516.

Figure captions

Fig. 1: Snapshots from molecular dynamics simulations (side and top view of the slabs) and density profiles (i.e., histogrammed densities of the electrolyte ions and water molecules in layers parallel to the surface, from the center of the slab across the interface into the gas phase) for 1.2 M aqueous HCl, HBr, NaOH, and NaCl. Coloring scheme: water oxygen, blue; hydronium oxygen, red; hydroxyl oxygen, pink; hydrogen, gray; sodium ions, green; chloride ions, yellow; bromide ions, orange.

Fig. 2: Density profiles of iodide from simulations of a 1.0 M solution of HI and NaI. Note the increased and shifted (towards the gas phase) interfacial peak in the acid. The Gibbs dividing surface is at ~23 A.

Fig. 3: Surface density (number per unit area) of free OH bonds (i.e., water OH bonds that are not hydrogen-bonded to another water molecule or ion) for neat water, HCl, HBr, NaOH, and NaCl, from the center of the slab to the surface.

Fig. 4: Vibrational sum frequency (ssp polarized) spectra of air/solution interfaces in the OH stretching region of neat water, 1.2 M NaCl, NaOH, HCl, HBr, and HI. Inset: Expanded view of the free OH region for neat water, 1.2 M HCl, and HBr (standard deviations shown as error bars).

Fig. 5: Probability densities of hydronium orientations from molecular dynamics simulations of aqueous solutions of 1.2 M HCl and HBr. Here θ is defined as the angle between the hydronium dipole moment (which points from the oxygen atom to the center of geometry of the hydrogen atoms) and a vector normal to the air-solution interface, and z is the location in the slab (z = 0 corresponds to the middle of the slab). The distributions are for the most part uniform (indicating isotropic orientational distributions), except for the pronounced peaks at $\cos\theta = -1$ and z ~ 14-15 Å, which correspond to hydronium ions strongly oriented at the air-solution interface with their dipoles pointing toward the interior of the solution.

Fig. 6: Comparison of density profiles of a) a single hydrated proton described using the quantum hopping method and sodium; b) polarizable and non-polarizable hydronium described using a classical force field.

Fig. 1 (Jungwirth et al.)

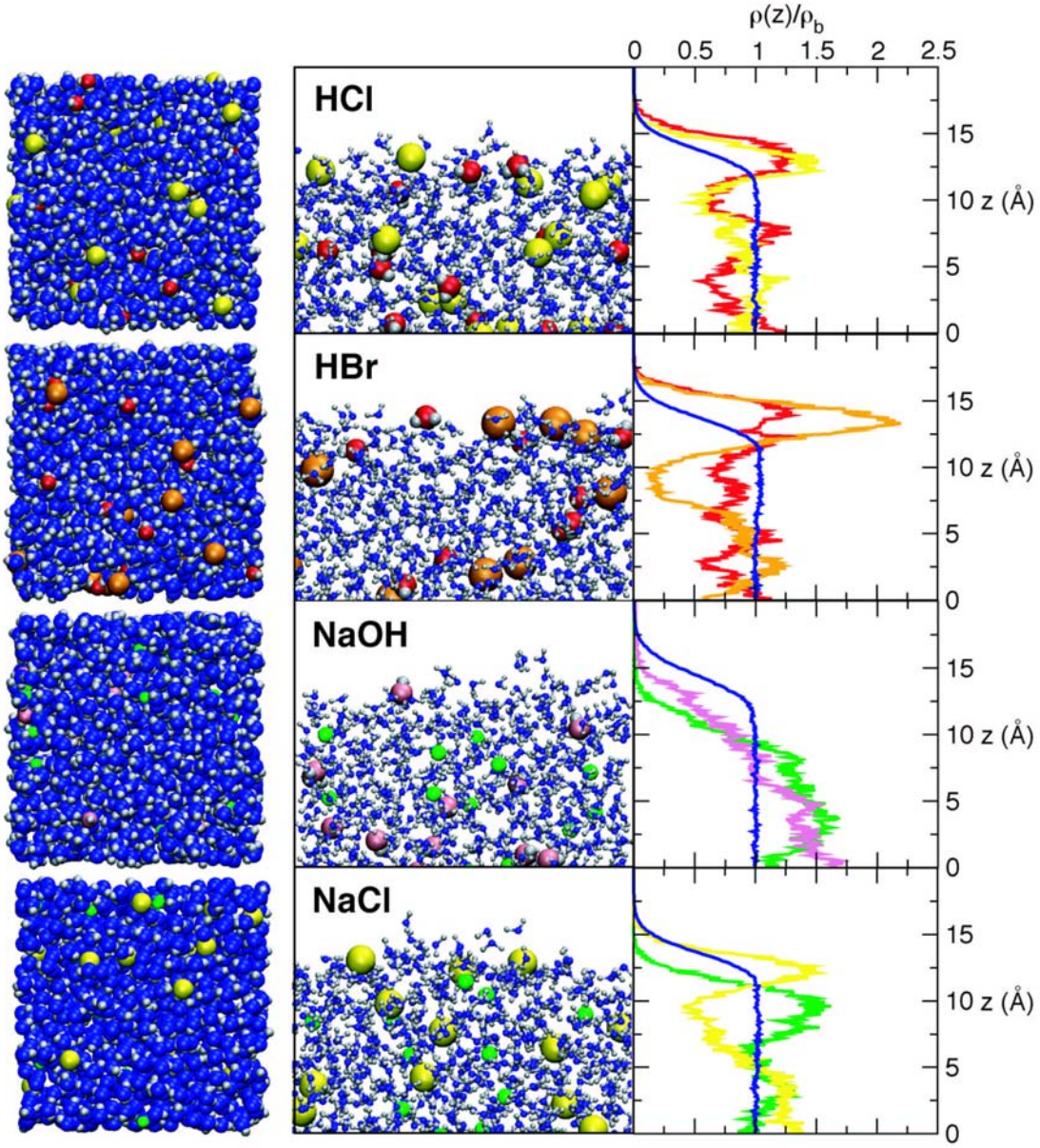

Fig. 2 (Jungwirth et al.)

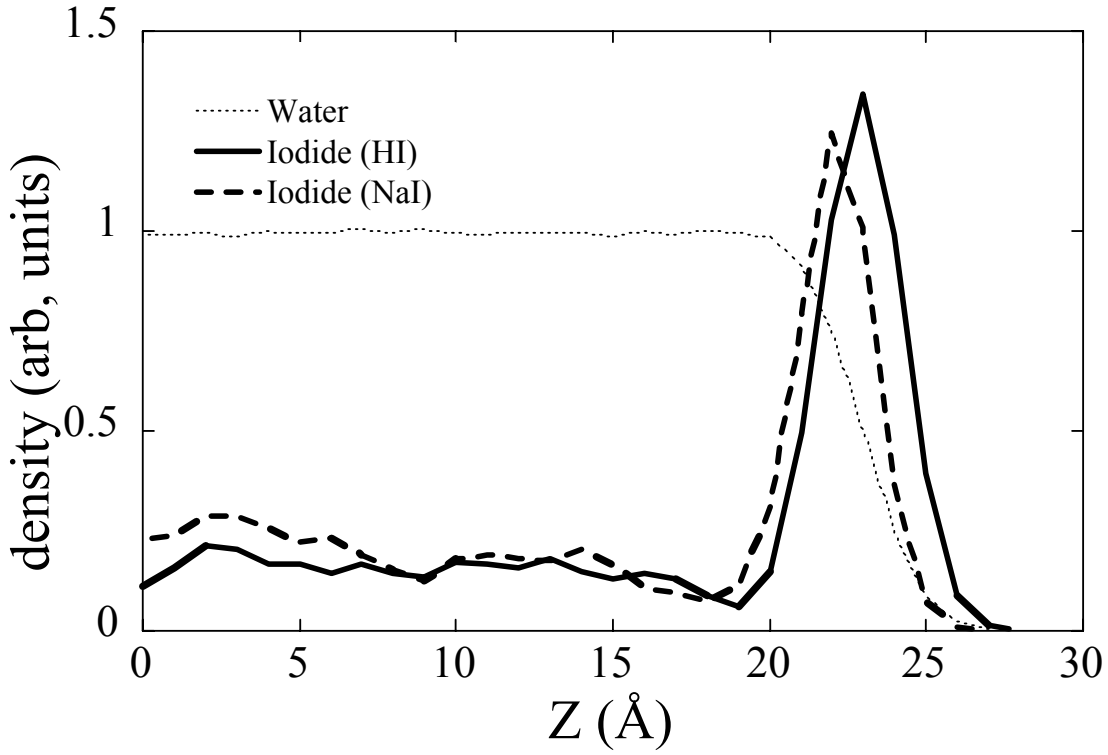

Fig. 3 (Jungwirth et al.)

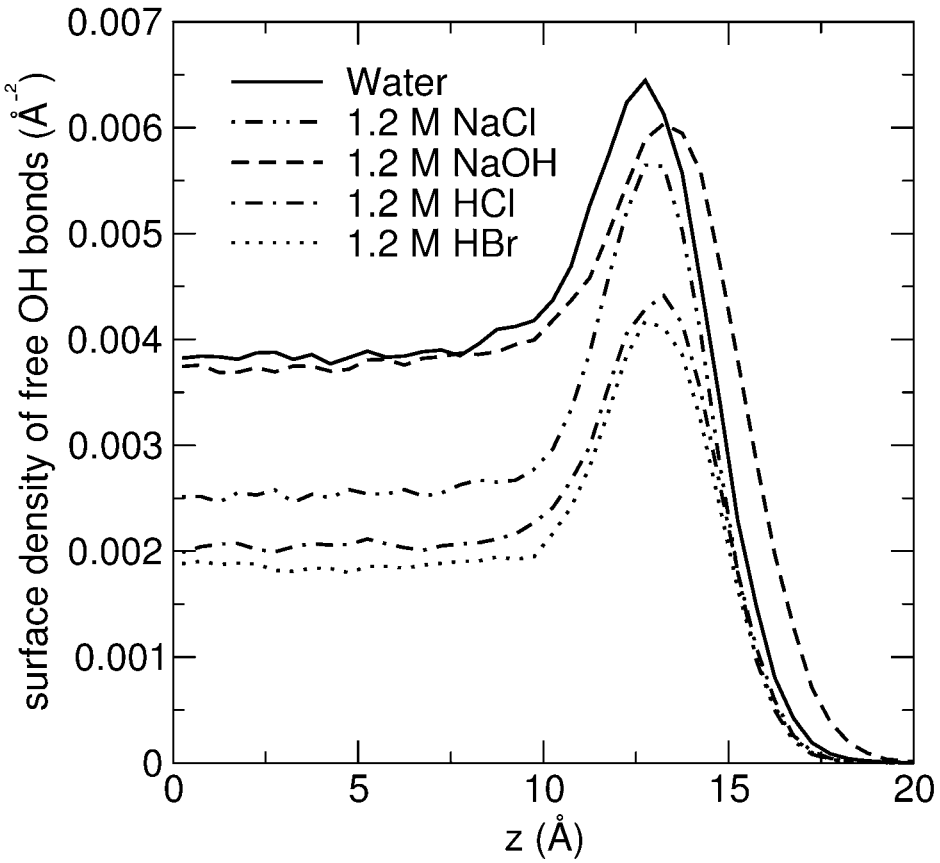

Fig. 4 (Jungwirth et al.)

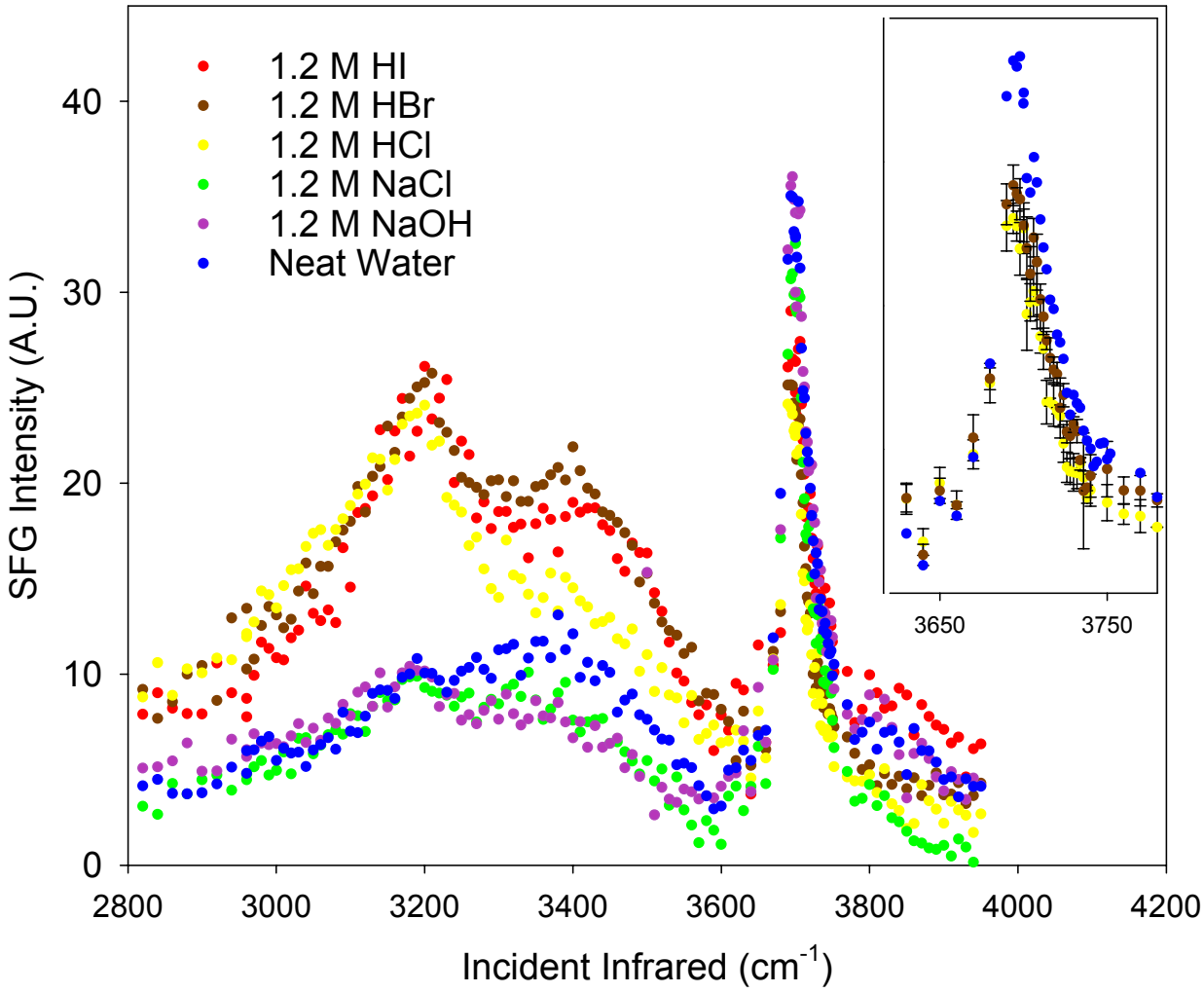

Fig. 5 (Jungwirth et al.)

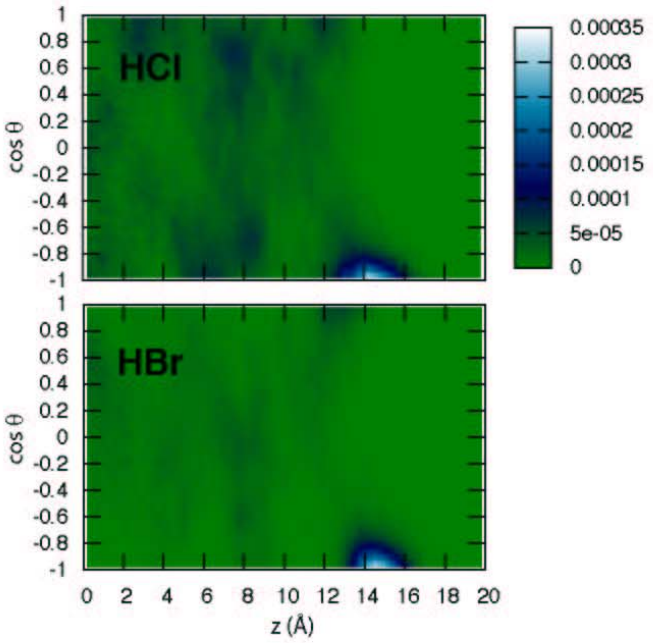

Fig. 6a (Jungwirth et al.)

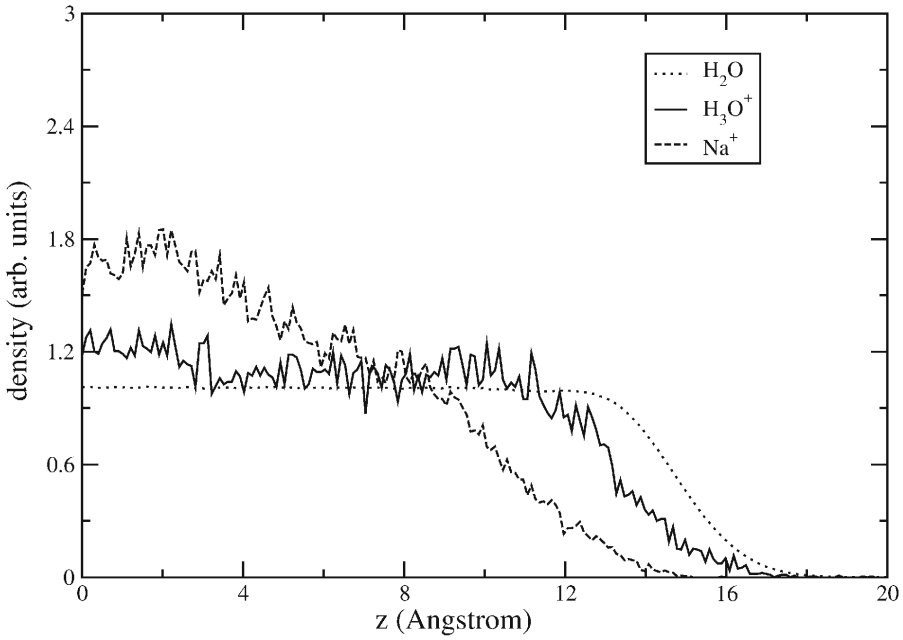

Fig. 6b (Jungwirth et al.)